

# Effects of asteroid rotation on directed energy deflection

Isabella E. Johansson<sup>a</sup>, Tatiana Tsareva<sup>b</sup>, Janelle Griswold<sup>b</sup>, Philip Lubin<sup>c</sup>, Gary B. Hughes<sup>d</sup>, Hugh O'Neill<sup>e</sup>, Peter Meinhold<sup>c</sup>, Jonathan Suen<sup>c</sup>, Qicheng Zhang<sup>c</sup>, Jordan Riley<sup>c</sup>, Carl Melis<sup>f</sup>, Kevin Walsh<sup>g</sup>, Travis Brashears<sup>c</sup>, Justin Bollag<sup>c</sup>, Shana Mathew<sup>c</sup> and Johanna Bible<sup>c</sup>.

[iej2106@columbia.edu](mailto:iej2106@columbia.edu)

[lubin@deepspace.ucsb.edu](mailto:lubin@deepspace.ucsb.edu)

<sup>a</sup>Columbia University, New York, NY 10027

<sup>b</sup>Santa Barbara City College, Santa Barbara, CA 93109

<sup>c</sup>Physics Department, University of California, Santa Barbara, CA 93106-9530

<sup>d</sup>Statistics Department, California Polytechnic State University, San Luis Obispo, CA 93407-0405

<sup>e</sup>Physics Department, California Polytechnic State University, San Luis Obispo, CA 93407-0405

<sup>f</sup>Center for Astrophysics and Space Sciences, UC San Diego, San Diego, CA 92093

<sup>g</sup>Southwest Research Institute, Boulder, CO 80302

## ABSTRACT

Asteroids that threaten Earth could be deflected from their orbits using laser directed energy or concentrated solar energy to vaporize the surface; the ejected plume would create a reaction thrust that pushes the object away from its collision course with Earth. One concern regarding directed energy deflection approaches is that asteroids rotate as they orbit the Sun. Asteroid rotation reduces the average thrust and changes the thrust vector imparting a time profile to the thrust. A directed energy system must deliver sufficient flux to evaporate surface material even when the asteroid is rotating. Required flux levels depend on surface material composition and albedo, thermal and bulk mechanical properties of the asteroid, and asteroid rotation rate. In the present work we present results of simulations for directed energy ejecta-plume asteroid threat mitigation. We use the observed distribution of asteroid rotational rates, along with a range of material and mechanical properties, as input to a thermal-physical model of plume generation. We calculate the expected thrust profile for rotating objects. Standoff directed energy schemes that deliver at least 10 MW/m<sup>2</sup> generate significant thrust for all but the highest conceivable rotation rates.

**Keywords:** DE-STAR, DE-STARLITE, Directed Energy, Laser Phased Array, Planetary Defense, Rotation Periods, COMSOL Multiphysics, Asteroid Rotation, Thermal Conduction, Thermal Inertia, the Yarkovski Effect

## 1. INTRODUCTION

Recent advances in the field of photonics have made a scientific discussion of directed energy planetary defense worthwhile. An orbital planetary defense system is proposed which would be capable of heating the surface of potentially hazardous objects to the point of vaporization as a feasible approach to impact risk mitigation. Vaporization of the target asteroid produces a plume of ejecta which generates thrust capable of diverting the asteroid from its earth-threatening orbit.

In the present paper we present results of calculations and simulations of such a system, taking into account realistic asteroid thermal properties, composition, rotation rates and masses. The paper is arranged as follows. In section 2 we outline some basic mission concepts. Section 3 presents basic asteroid properties relevant to the analysis. In section 4 we describe and compare 3 methods of estimating the thrust generated by DE-STAR on model asteroids, with progressively more realistic inputs. Section 5 presents calculations and simulations of the deflection of asteroid trajectories.

## 2. MISSION CONCEPTS

### 2.1. DE-STAR

The system analyzed in this paper is called **DE-STAR** for **Directed Energy System for Targeting of Asteroids and exploRation**.<sup>1</sup> Scaling of laser technology has propelled development of directed energy systems, which are capable of delivering high flux on target sufficient to vaporize any known material. A critical point for this program is that such devices can be phase locked, allowing more efficient delivery of energy to distant targets. The proposed system consists

of an array of phase-locked, kW class laser power amplifiers driven by a common seed laser. By controlling the relative phases of individual laser amplifier elements, the combined beam can be directed to a distant target. The lasers are powered by solar photovoltaics of essentially the same area as the laser array. By increasing the array, it is possible to both reduce the spot size due to diffraction and increase the power. This dual effect allows the system to vaporize elements on the surface of asteroids at distances that are a significant fraction of the size of the solar system. The flux on target ( $W/m^2$ ) at a fixed distance scales by  $d^4$  where  $d$  is the linear dimension of the laser array and thus it increases very rapidly with increased array size.<sup>1</sup>

By raising the flux on the target asteroid to a sufficiently high level, the system can begin direct evaporation of the asteroid at the focused spot. Evaporation at the spot creates a back reaction on the asteroid from the vaporization plume, which acts as a rocket and the asteroid can be deflected. It is convenient to classify a DE-STAR system by the log of its linear size: a DE-STAR 1 is 10 m, DE-STAR 2 is 100 m, *etc.* A DE-STAR 4 system will produce a reaction thrust comparable to the shuttle solid rocket booster (SRB) in terms of thrust per watt of input power, on an asteroid at 1 AU [AU = Astronomical Unit =  $\sim 1.5 \times 10^{11}$  m]. The thrust created by mass ejection allows for orbital deflection of even very large asteroids, exceeding several kilometers in diameter, allowing for protection from every known asteroid threat. Smaller systems are also extremely useful. For example, a DE-STAR 2 (100 m size array - roughly the size of the ISS) would be capable of diverting volatile-laden objects 100 m in diameter by initiating engagement at  $\sim 0.01$ -0.5 AU. Smaller objects could be diverted on shorter notice. The phased array configuration is capable of creating multiple beams, so a single DE-STAR of sufficient size could engage several threats simultaneously, such as a Shoemaker-Levy 9 scenario (a large asteroid breaking into multiple dangerous units) impacting Earth.

## 2.2. DE-STARLITE – JPL ARM Mission

While the primary motivation for DE-STAR has been as a "standoff" planetary defense system, the same laser array concept can be used in a variety of ways. The directed beam can be used for composition detection or even mining of asteroids, the moon or Mars. A miniature system can be brought close to a target to enable any of these capabilities. An example of this is the DE-STARLITE mission where a small (1-100 kW) system is brought near to the asteroid and mass ejection is initiated to change the asteroid's orbit.

The advantage of the amplified laser system over a simple mirror focusing sunlight on the asteroid is that the mirror must have an  $F\# < 2$  to be effective on high temperature rocky compounds. This requires getting the mirror extremely close to the asteroid (typically 10-100 m away). The reason the  $F\#$  has to be so low, for a mirror, is that the sun is not a point source and thus the flux on target  $I_T$  ( $W/m^2$ ) is the flux at the surface of the sun divided by 4 times the  $F\#^2$  thus  $I_T = I_{sun} / 4F\#^2$ . The flux at the surface of the sun is about  $60 MW/m^2$  and thus with an  $F\# = 2$  mirror the spot flux on the target would be about  $4 MW/m^2$  which is just barely enough to start significant evaporation of rocky materials unless there are significant volatiles present. An  $F\# = 1$  mirror would be much preferred in this case. This is the same reason a simple mirror at the Earth will not evaporate distant asteroids unless the mirror diameter is roughly the size of the distance to the target (*i.e.*, 1 AU mirror diameter!). While using mirrors close to an asteroid is not impossible, the close proximity can cause severe optical pitting and dust buildup on the mirror. DE-STARLITE can standoff some 1-100 km away from the target and does not require sun-target alignment allowing much more flexible steering. DE-STARLITE can also run pulsed if needed for more flexible mission scenarios. **In all of these cases, the asteroid material is converted into its own propellant offering a much more efficient and powerful thruster than an ion engine of equivalent power and needs no propellant other than the asteroid itself.**

Studies to date indicate that Apophis class asteroids (325 m diameter) can be deflected with a dedicated mission using less than 100 kW of power with a decade of time on target. Since the asteroid itself is the "rocket fuel" such a mission does not suffer from having to take up a very large fuel load as would be required by an approach that uses ion engines only. A combined mission with ion engines for transport of the laser to the target and use of the ion engines for station keeping looks feasible with an Atlas or Ariane V or the upcoming SLS (Space Launch System). As a specific example, the deflection of a 325 m diameter asteroid (like Apophis) is studied, assuming a DE-STARLITE stand-on mission with the laser on for 15 years with a reasonable Earth crossing orbit. A force of 2 N over 10 years is sufficient to cause a 2 Earth-radius miss distance.<sup>2</sup>

### 3. NEAR EARTH ASTEROID CHARACTERISTICS

#### 3.1. Understanding Rotation Periods

Asteroids do rotate, but generally quite slowly. A complete picture of rotation properties is not available, but from the limited data collected on the rotation of larger bodies and the break up speed it is estimated that asteroids in the 0.1-1 km class typically rotate no faster than once per several hours; see Fig. 1. Results of detailed observation indicate the rotation properties for more than 6,000 significantly rotating asteroids and conclude that rotation is not an issue in general as larger asteroids (>150 m) are typically largely gravitational bound "rubble piles" and for these the maximum rotation is independent of diameter and only depends on density  $\rho$ , with an angular speed  $\omega$ , and rotation period  $\tau$  given by:

$$\omega = \sqrt{\frac{4}{3}\pi G\rho} = \frac{2\pi}{\tau}, \quad \tau = \sqrt{\frac{3\pi}{G\rho}} \quad (2.1)$$

$$\tau \approx 1.19 \times 10^4 \rho[\text{g/cc}]^{-1/2} \text{s} \approx 3.3 \rho^{-1/2} [\text{hr}], \text{ independent of diameter.} \quad (2.2)$$

Estimated densities are in the range of  $\rho \sim 2$  [g/cc] yielding a minimum rotation period of about 2.3 hours. This is clearly seen in Fig. 1.

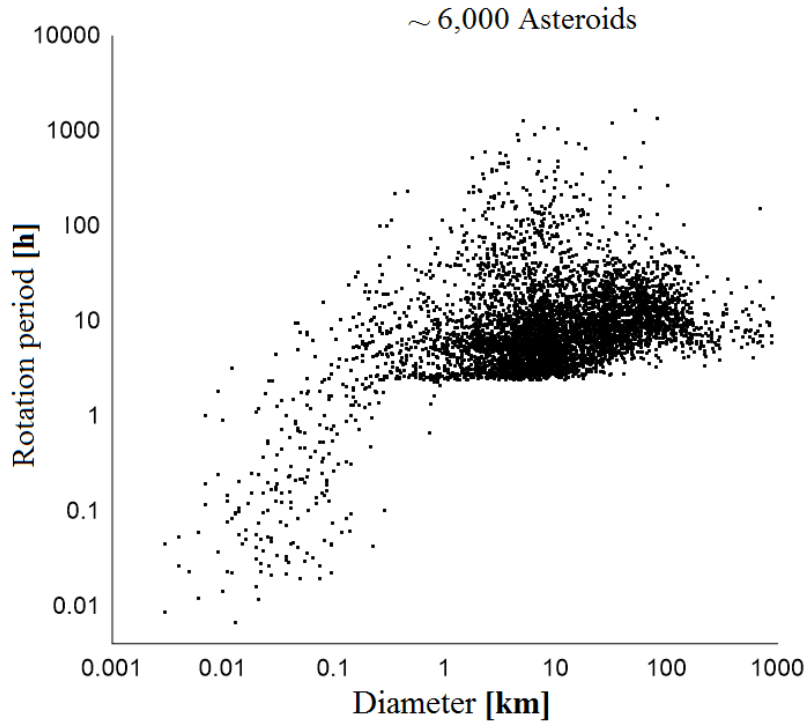


**Figure 1.** Measured rotation period of ~6,000 asteroids. A distribution of measured asteroid rotation rates, notice the very sharp cutoff at just above 2 hours for larger diameter asteroids. Data from Minor Planet Center.<sup>3</sup> The superfast rotators, those at the lower left with periods < 2.2 hours and  $D < 0.1$  km are likely molecularly bound and form a distinct population.

The cutoff in rotation periods is observed to be remarkably sharp (see figure 1), and lies very close to 2 hours for asteroids of diameters greater than approximately 150 m, consistent with equation 2.1. Some smaller asteroids can rotate faster as they can have a tighter binding than purely gravitational (such as an iron meteorite) but these are relatively rare.

Even fast rotating asteroids can be dealt with since the mass ejection begins so quickly after the laser is turned on. As is seen in the transient thermal simulations below, the mass ejection and hence thrust begin within about 1 second for a DE-STAR 4 at 1 AU. It is largely a flux issue so that for the same flux at any distance the mass ejection remains at this rate. This is assuming an asteroid consisting of solid  $\text{SiO}_2$ , which is extremely conservative. Loss is included to mimic

the absorption qualities of asteroids, which are very absorptive having typical reflection coefficients around 5-10%. Thus, a rotating asteroid with this rate (1 hour) poses little problem. More interesting perhaps would be an attempt to spin up (or down) an asteroid depending on beam placement as discussed below.

### 3.2. The Yarkovsky-O'Keefe-Radzievskii-Paddack (YORP) Effect

The spin rate of asteroids can either increase or decrease by means of a propulsion effect due to thermal re-emission of photons on the surface of an asteroid known as the Yarkovsky-O'Keefe-Radzievskii-Paddack (YORP) effect, a non-gravitational effect. The overall propulsion force causes a net torque, which ultimately can change the period of rotation and direction of rotation axis. The force applied onto the asteroid is quite small, but the accumulation of this ongoing process over time can result in a very large rotation rate change. Asteroids which rotate in the same direction as their orbit, prograde rotators, are driven in the same direction of orbit and therefore the spin rate is increased due to the Yarkovsky effect. Asteroids with a retrograde rotation are pushed in a backward direction as a result of the Yarkovsky effect, slowing down the spin. The asteroid 1862 Apollo, diameter of 1,400 km, has been observed to increase in one additional orbit rotation cycle over the last 40 years, resulting in a decrease in its orbit rotation period. From the changes of the spin rate and orbit rotation period, speculations that the YORP effect causes structural alterations on the surface due to mass shedding, removing angular momentum. Many factors must be taken into consideration such as size, shape, spin, mass in the process of predicting changes in momentum.

Observed changes in spinning rates are in reasonable agreement with theoretical calculations<sup>7</sup>, and the effect explains the anomalous distribution of spin rates for asteroids under 10 km in diameter. Thermal conductivity of compounds in the asteroid surface composition is also a factor in the resulting outcome of the Yarkovsky effect. If the spin rate and shape are known, the Yarkovsky effect could be used to model accurate trajectories and through observation of the strength of the YORP effect, it is also possible to estimate the mass (density) of small asteroids given that the shape and size are known sufficiently well.

## 4. THERMAL ANALYSIS AND CURRENT MODELS

We calculate the thrust produced by DE-STAR on an asteroid using three different modeling approaches, of increasing complexity and realism. We present and compare results from the three analyses, which all yield consistent answers. The basic equations are derived from energy conservation:

$$\text{Power in (laser)} = \text{Power out (radiation + mass ejection)} + \frac{dU}{dt}$$

Where U= Asteroid internal energy and  $\frac{dU}{dt}$  is effectively from conduction.

$$\text{In the steady state } \frac{dU}{dt} = 0$$

$$P_{\text{in}} = P_{\text{out}} + \frac{dU}{dt}, \text{ with } U = \int \rho c_v dv \quad (3.1)$$

Where  $c_v$  = specific heat [J/kg-K],

$F_L$  = Laser flux [ $\text{W}/\text{m}^2$ ] - (in),  $F_{\text{cond}}$  = Thermal conduction [ $\text{W}/\text{m}^2$ ] - (in), and

$F_{\text{rad}}$  = Radiation flux [ $\text{W}/\text{m}^2$ ] - (out),  $F_{\text{ejecta}}$  = Ejecta flux [ $\text{W}/\text{m}^2$ ] - (out).

Assuming  $P_{\text{in}} = P_{\text{rad}} + P_{\text{ejecta}} + P_{\text{cond}}$ , then:

$$\oiint (F_L - \bar{F}_{\text{rad}} - \bar{F}_{\text{ejecta}} - \bar{F}_{\text{cond}}) \cdot \hat{n} dA = 0 \quad (3.2)$$

$$\text{or } = \int \nabla \cdot (\bar{F}_L - \bar{F}_{\text{rad}} - \bar{F}_{\text{ejecta}} - \bar{F}_{\text{cond}}) dV = 0 \quad (3.3)$$

Locally:

$$\vec{F}_L = \vec{F}_{\text{rad}} + \vec{F}_{\text{Ejecta}} + \vec{F}_{\text{cond}} \quad (3.4)$$

$$\vec{F}_{\text{rad}} = \sigma T^4 \hat{n} \quad (3.5)$$

$$\vec{F}_{\text{Ejecta}} = \Gamma e H_v \hat{n} = M^{1/2} (2\pi RT)^{-1/2} \alpha_e 10^{[A-B/(T+C)]} H_v \hat{n} \quad (3.6)$$

$$\left| \vec{F}_{\text{cond}} \right| = K \nabla T, \quad (3.7)$$

$$\left| \vec{F}_{\text{rad}} \right| = \sigma T^4, \text{ and } \left| \vec{F}_{\text{Ejecta}} \right| = \Gamma e \cdot H_v.$$

Where K is the thermal conductivity (which can be position and temperature dependent) and  $\Gamma e$  is the mass ejection flux [kg/m<sup>2</sup>-s], and  $H_v$  is the heat of vaporization [J/kg]. The heat of fusion,  $H_f$ , is included for relevant cases. The heat of fusion is sometimes referred to the heat of sublimation as is sometimes the case for compounds in vacuum.  $H_f$  is typically a small fraction of  $H_v$ . The mass ejection flux is shown in equation 3.8 which uses vapor pressure.

$$\Gamma e = \frac{M \alpha_e (P_v - P_h)}{\sqrt{2\pi MRT}} = M^{1/2} (2\pi RT)^{-1/2} \alpha_e (P_v - P_h) \quad (3.8)$$

M = Molar mass [kg / mol]

$P_v$  = Vapor pressure [Pa]

$P_h$  = Ambient vapor pressure = 0 (in vacuum)

$\alpha_e$  = coef. of evaporation

The models vapor pressure for each element and compound is determined using a semi analytic form known as Antoine coefficients A, B and C in equation 3.9.

$$\text{LOG}(P_v) = A - B / (T + C) \quad (3.9)$$

Where A, B and C are unique per element and compound. Hence:

$$P_v = 10^{[A-B/(T+C)]} \text{ and } \left| \vec{F}_{\text{Ejecta}} \right| = M^{1/2} \frac{1}{\sqrt{2\pi RT}} \alpha_e 10^{[A-B/(T+C)]} H_v \quad (3.10)$$

A Gaussian profile is assumed for the laser as an approximation shown in equation 3.11 where the Gaussian laser power is  $P_T$ , and r is the distance from the spot center.

$$\left| \vec{F}_L \right| = \frac{P_T}{2\pi\sigma^2} e^{-r^2/2\sigma^2}$$

In the approximation where the spot is small compared to the asteroid, the equation becomes:

$$\vec{F}_L = \frac{-P_T}{2\pi\sigma^2} e^{-r^2/2\sigma^2} \hat{n} \quad (3.11)$$

In the dynamic case it is possible to solve for transient heat flow by :

$$\nabla \cdot (K\nabla T) + \frac{d}{dt}(\rho c_v T) = 0 \quad (3.12)$$

$$K\nabla^2 T + \rho c_v \frac{dT}{dt} = 0 \quad (3.13)$$

In equation (3.16) it is assumed that **K** (thermal conductivity) is independent of position,  $\rho$  and  $c_v$  are time independent. In the full 3D time dependent solution, all of the above conditions are invoked and the equations are solved simultaneously using a 3D numeric solver (COMSOL in this case). In the 2D steady state solutions, the thermal conductivity is assumed to be small (this is shown in 3D simulations to be a valid assumption as well as from first principle calculations) and a combination of radiation and mass ejection (phase change) is used:

$$|\overline{F}_L| = |\overline{F}_{rad}| + |\overline{F}_{Ejecta}| = F_T \quad (3.14)$$

$$F_T = \sigma T^4 + M^{1/2} (2\pi RT)^{-1/2} 10^{[A-B/(T+C)]} H_v \quad (3.15)$$

Inversion is not analytically tractable so numerical inversion is used to get  $T(F_T)$  which gives  $P_v(F_T)$ ,  $\Gamma_e(F_T)$  etc. In this inversion, a function fit is found (to 10th order typically);

$$T = \sum_{n=1}^N a_n (\log F_T)^n \quad (3.16)$$

A Gaussian approximation to the laser profile is used (this is not critical) to get  $T(r)$ ,  $P_v(r)$ ,  $\Gamma_e(r)$  where  $r$  is the distance from the center of the spot.

Since radiation goes as the 4<sup>th</sup> power of  $T$ , while the mass ejection from evaporation goes roughly exponentially in  $T$ , at low flux levels the outward flow is completely dominated by radiation (the asteroid is heated slightly and it radiates). As the spot flux level increases (spot size shrinks or power increases or both) evaporation becomes increasingly dominant and eventually at about  $T \sim 2,000-3,000$  K or fluxes of  $10^6 - 10^7$  W/m<sup>2</sup> mass ejection by evaporation becomes the dominant outward power flow and (just as water boiling on a stove) the temperature stabilizes and increasing flux only increases the rate of mass ejection with only very small increases in temperature.<sup>1</sup>

The three methods:

- **1D Energetics alone.** Use heat of vaporization and set spot flux to correspond  $T \sim 6,000$  K IF the system were completely radiation dominated. No radiation or conduction included, only vaporization.
- **2D Analytic** - Model elements and compound vapor pressure vs.  $T$ . Include radiation emission. Ignore thermal conduction
- **3D Numeric** - Full 3D FEA include phase change, vapor pressure, mass ejection, radiation and thermal conduction

#### 4.1. 1D Energetics Alone

The heat of vaporization of a compound is the energy (*per mole or per kg*) to remove it from the bulk. Removal energy is related to an effective speed and an effective temperature, which are related to but somewhat different than the physical speed of ejection and the physical temperature of vaporization. To be more precise, the term evaporation refers to molecules or atoms escaping from the material (*for example water evaporating*), while boiling is the point at which the vapor pressure equals or exceeds the ambient pressure. At any non-zero temperature, there is a probability of escape from the surface: evaporation happens at all temperatures and hence vapor pressure is a quantitative measure of the rate of evaporation. The heat of vaporization is also temperature and pressure dependent to some extent. Table 1 gives thermal properties for various materials in asteroids. These materials have relatively high effective temperatures reflecting the fact that there is a probability distribution of energies and an increase in vapor pressure with respect to Temperature.<sup>1</sup>

Material	$H_f$ [kJ/mol]	$H_v$ [kJ/mol]	$M$ [g/mol]	$H_v$ [ $10^6$ J/kg]	$C_v$ [J/kg-K]	$V_{eff}$ [km/s]	$T_{eff}$ [ $10^4$ K]
<b>SiO2</b>	<b>9.0</b>	<b>143</b>	<b>60.1</b>	<b>2.38</b>	<b>730</b>	<b>1.54</b>	<b>0.573</b>
Al2O3	14.2	293	102.0	2.87	930	1.69	1.15
MgO	77.4	331	40.3	8.21	1030	2.87	1.32
ZnS	38.0	320	97.5	2.46	472	1.57	1.28

**Table 1.** List of thermo-physical properties of common high temperature asteroid compounds. Here  $H_f$  is the heat of fusion and  $H_v$  is the heat of vaporization.  $v_{eff} = H_v^{1/2}$  [J/kg] and  $T_{eff} = (M \cdot H_v) / 3R$  where  $R = k \cdot N_A \sim 8.31$

The thermal probability distribution has a "tail" allowing for escape from the surface at lower temperatures than one would naively conclude from a mean analysis only. If power  $P_T$  from the laser impinges on the asteroid in a small enough spot to heat to above the radiation dominated point (typically 2,000-3,000 K for "rocky" asteroids vs. 300-500 K for comets) it is possible to compute the evaporation flux (mass ejection rate) as:  $M_e = P_T / H_v$ . This is the maximum possible rate of mass ejection. It is possible to get quite close to this maximum if the system is designed properly.

#### 4.2. 2D Analytic

As mentioned above, this calculation assumes that the thermal conduction is small compared to radiation and mass ejection (a good assumption for most asteroids). Using the equations above and the numerical inversions it is possible to solve for the temperature distribution and thus the mass ejection and thrust on the asteroid among many other parameters. A summary is shown in Fig. 2 for SiO<sub>2</sub>. The parameter  $\sigma$  (sigma) in the Gaussian beam profile is allowed to vary to show the effects of non-ideal beam formation as well as beam and pointing jitter. The diffraction-limited  $\sigma$  at 1 AU should be about 5 m for a DE-STAR 4. As can be seen the system is quite tolerant to errors in beam formation, focus, beam jitter and pointing errors even beyond  $10\sigma$  as long as the power is high enough. The requirements on a low power system at equivalent distances are more severe. These relationships also show that it is possible to nearly achieve the theoretical maximum mass ejection rate. Also, note the thrust (N) per Watt is close to 0.001 N/W for the 1,000 kW case. This is comparable to the Shuttle SRB in thrust per watt. This is not really surprising, considering that conventional propellants are approximately thermal in nature with temperatures close to the maximum sustainable in the combustion chamber and exhaust nozzle (i.e., a few  $\times 10^3$  K).

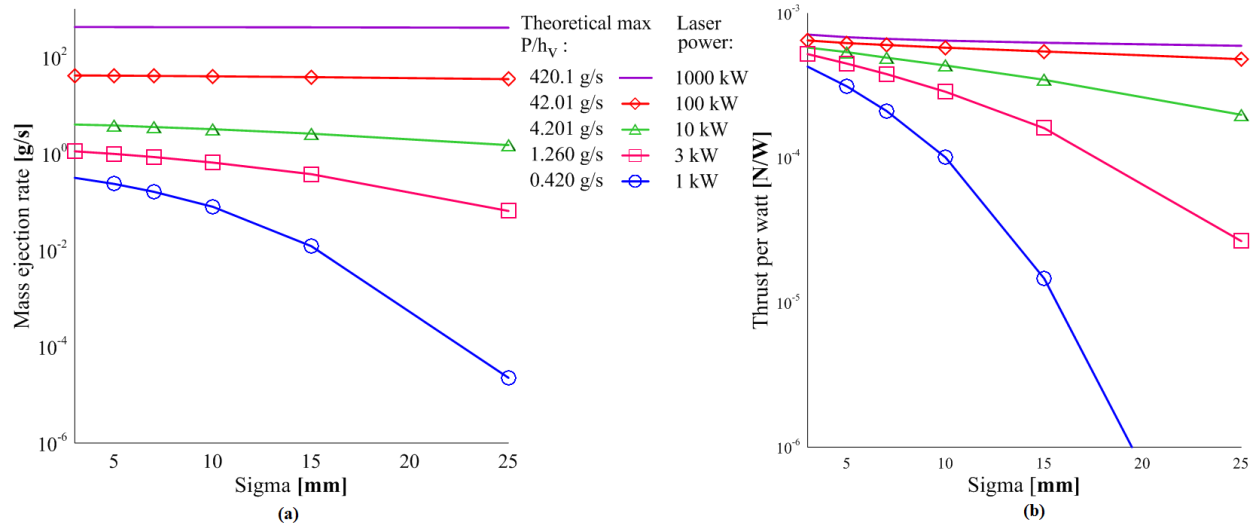


**Figure 2.** Using SiO<sub>2</sub> as the equivalent material. (a) Integrated mass ejection rates vs. sigma case for different powers between 1 kW and 1 MW. (b) Similarly, integrated thrust (N) per watt vs. sigma

#### 4.3. 3D Numeric Calculations and Simulations

Thousands of 3D model simulations have been run, and a few salient results are apparent. Calculations based on the simplest assumptions, namely energetics, and the conservation of spot flux, were validated. The more sophisticated tools are needed for further analysis and optimization of the system. For the case of dynamic targeting and rotating objects, time evolution has been added to the 3D solver. Some of this is motivated by the need to understand the time evolution

of the mass ejection under dynamic situations. This is partially shown in Fig. 3 where the time evolution of the temperature at the center of the spot is shown. It is now possible to simulate full dynamics and apply this to the case of rotating asteroids. The same techniques can be applied to pointing jitter and "laser machining" of the asteroid or other target.

The time evolution of the heated spot is shown in Fig. 4. Again, all cases refer to SiO<sub>2</sub> as the equivalent material for an asteroid. DE-STARLITE (as a stand-on system) is modeled here with a 1 m laser array, with a Gaussian beam and a total optical power of 1 MW, and spot diameter ~ 30 mm ( $\sigma \sim 5$  mm).

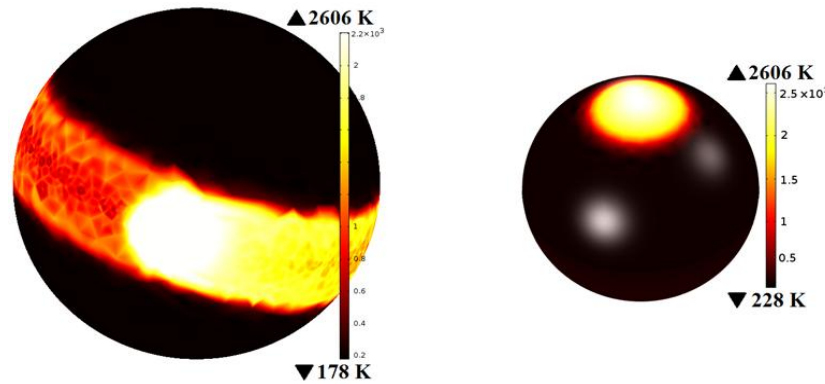


**Figure 3.** Rotating and stationary 3D plots for SiO<sub>2</sub>: Using 1 hour rotation period for a 100 m diameter asteroid with 50 GW laser power (DE-STAR 4) at 1 AU, yields equal surface temperature distribution as in the stationary steady state case. Temperatures rise to the point of being mass ejection limited, which is about 2,600 K in the center of the spot. Solar illumination is modeled with an isotropic average of 350 W/m<sup>2</sup>.

**Video 1:** <http://dx.doi.org/doi.number.goes.here>

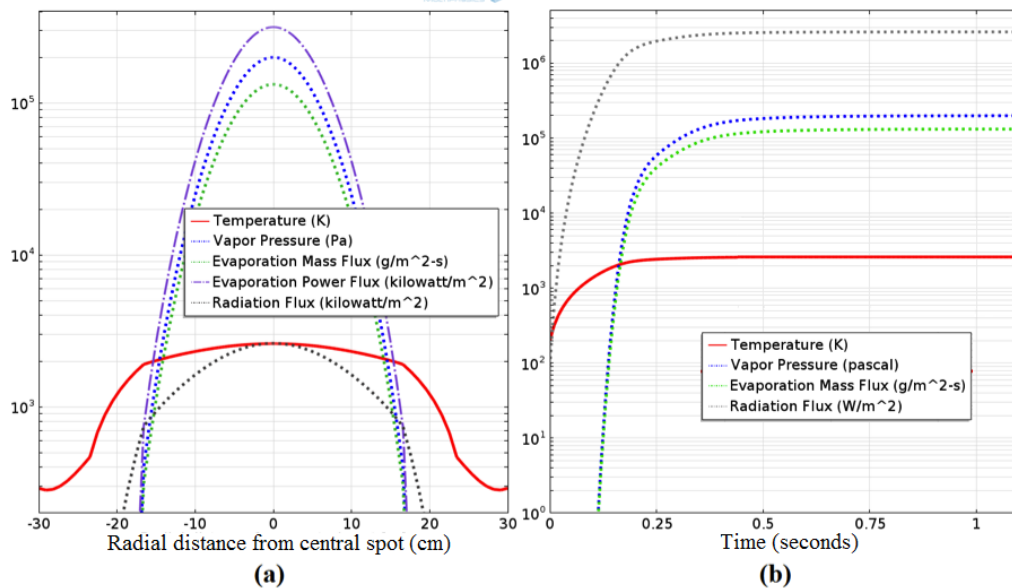


**Figure 4.** (a) Temperature, vapor pressure and mass loss distribution vs. distance from center (angle from beam axis). High frequency sub structure is due to numerical meshing. (b) Transient time solution (stationary) of temperature in the spot center (K) vs. Time (seconds) after the laser is turned on at  $t = 0$ . Initial temperature is 200 K. Mass ejection begins within 1 second.



#### 4.4. Comparing Results Among Models

While the 3D simulations give time transient solutions and include full thermal conduction, they lack the numerical flexibility of the 2D solutions. Results of the temperature distributions for a Gaussian laser illumination are compared, and found to be very close in their predictions. This builds confidence that it is possible to do both 2D and 3D simulations with high fidelity. Fig. 5 shows comparisons of Gaussian beam illuminations; results are nearly identical in the critical central region.

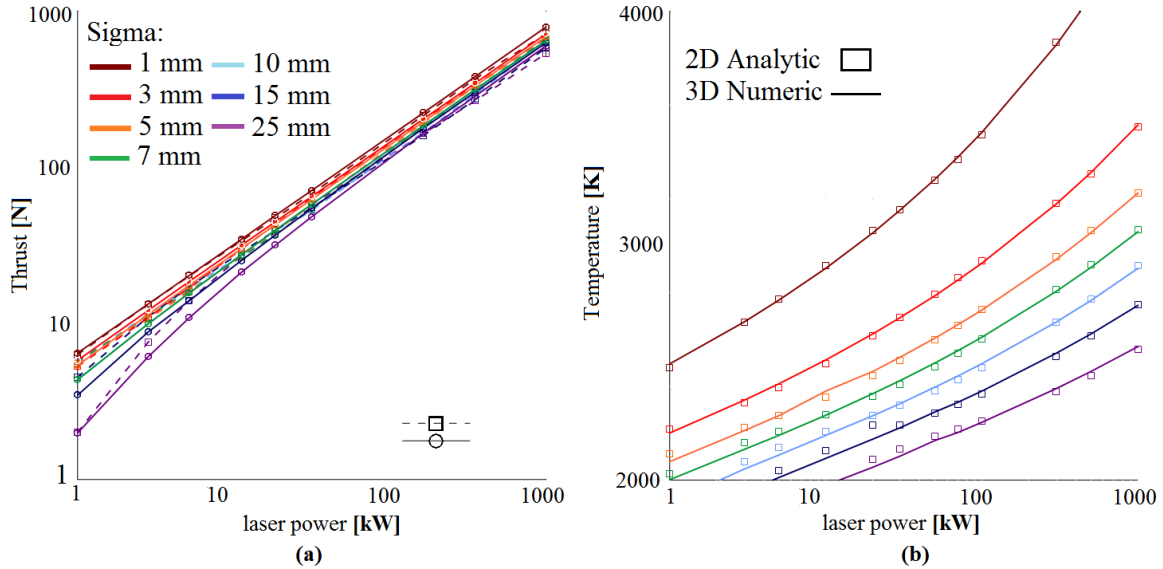


**Figure 5.** Comparison of 2- and 3-D models, hence numeric + analytic values for **(a)** integrated surface thrust (N) vs. total laser power for sigma between 1 and 25 mm. Note that the spot diameter ( $\sim 6\sigma$ ) for a DE-STARLITE kW class system is typically 3 to 75 mm. **(b)** Central spot temperatures. (In this case: DE-STARLINE – 1 m aperture)

The ultimate test will come when comparing model results with laboratory tests. As laboratory tests are refined, the results will feed back into the models for various materials.

#### 4.5. Thermal Conduction

Unfortunately it is not possible to bring asteroids into the laboratory to study their thermal properties, so it is necessary to rely on astronomical observations, primarily in the infrared, combined with assumptions about their formation and likely structure, to deduce their properties. Several references<sup>3,4,5,6</sup>, among many others, have done excellent work in this area and it is possible to use their results. One can derive the thermal properties by studying the time varying temperature as deduced from infrared observations. In this way the thermal inertia  $\Gamma$  ( $J/m^2-K-s^{1/2}$ ) and thermal conductivity  $K$  [ $W/m-K$ ] are derived.

The relationship between them is:

$$\Gamma = [\rho K C]^{1/2}$$

$$\rho = \text{Density [kg/m}^3\text{]}$$

$$C = \text{heat capacity [J/kg-K], hence:}$$

$$K = \Gamma^2 / (\rho \cdot C) \tag{3.17}$$

The data is shown in Fig 6 best fit to data<sup>6</sup>, where  $D$  is the asteroid diameter [km] is:

$$\Gamma = d \cdot D^{-\xi} \tag{3.18}$$

$$\text{With } d = 300 \text{ [km], } \xi = 0.4, \text{ and } K = 3e4 \cdot D^{-0.8} / (\rho \cdot C) \tag{3.19}$$

Typical value are  $\rho \sim 2000 \text{ kg/m}^3$  and  $C \sim 500 \text{ J/kg-K}$

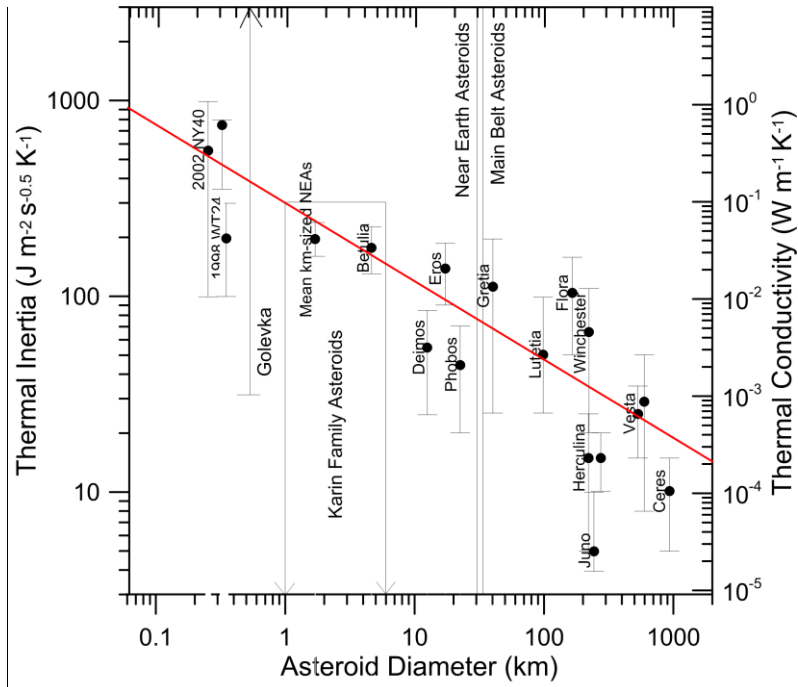


**Figure 6.** Thermal Inertia  $\Gamma$  - [ $\text{J/m}^2\text{-K}\cdot\text{s}^{1/2}$ ] and Thermal Conductivity:  $K$  - [ $\text{W/m}\cdot\text{K}$ ]

The trend (*with some significant deviations*) is towards smaller asteroids having larger thermal conductivity and larger asteroids having smaller thermal conductivity. Some of this may be the point contacts from "rock pile" effect for larger asteroids. A similar trend between asteroid size and thermal inertia is also observed. It is the values that are of interest in the models. A relatively conservative case of  $K = 1$  [ $\text{W/m}\cdot\text{K}$ ] is assumed. To put this in perspective, some values for common materials are given in Table 2.

Material	$K$ [ $\text{W/m}\cdot\text{K}$ ]	$\rho$ [ $\text{kg/m}^3$ ]	$C$ [ $\text{J/kg}\cdot\text{K}$ ]	$\Gamma$ [ $\text{J/m}^2\text{-K}\cdot\text{s}^{1/2}$ ]
Nickel	91	8850	448	$1.9 \times 10^4$
Iron	81	7860	452	$1.7 \times 10^4$
Granite	2.9	2750	890	2600
Ice (solid)	2.3	917	2000	2040
<b>SiO<sub>2</sub> (solid)</b>	<b>1.04 (at 200°C)</b>	<b>2200</b>	<b>1000</b>	<b>1510</b>
Water (liq 0°C)	0.56	1000	4200	1500
Snow (firm)	0.46	560	2100	740
Soil (sandy)	0.27	1650	800	600
Pumice	0.15	800	900 ( <i>varies significantly</i> )	330
Styrofoam	0.03	50	1500	47
Air	0.026	1.2	1000	5.6
Moon (regolith)	0.0029	1400	640	51

**Table 2.** Common material thermal properties for comparison to the asteroid thermal properties in Fig. 6

Increased thermal conductivity results in lower final spot temperatures of the asteroid target as shown in Fig. 5 even when laser power doubled. Raising laser power from 10 kW to 20 kW resulted in slightly smaller range between minimum and maximum final temperatures, and yet revealed a relatively small effect on the final temperature between the two laser powers. For these simulations, a relatively conservative case of  $K = 1$   $\text{W/m}\cdot\text{K}$  is assumed. For values of thermal conductivity between 0.01 and 250  $\text{W/m}\cdot\text{K}$ , the evaporation mass flux and thrust change only slightly, shown in Fig. 7.

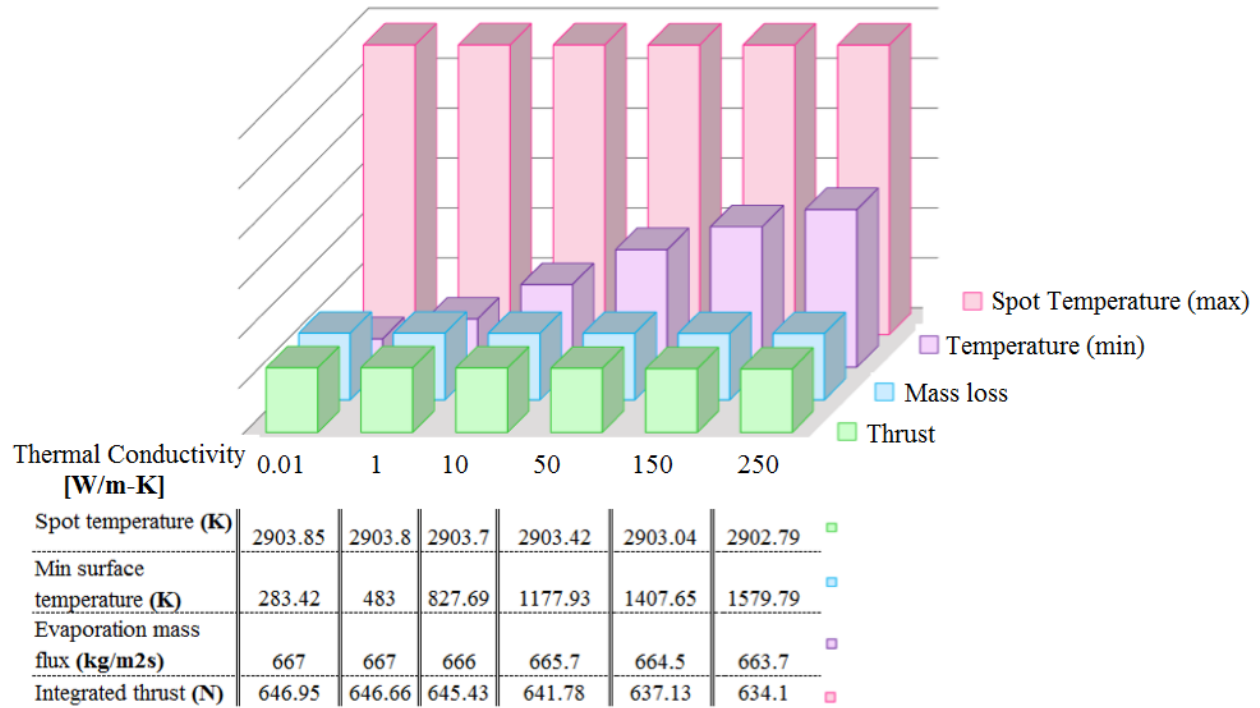


**Figure 7.** Extreme values inputs of thermal conductivity set to 0.01-250 W/m-K for SiO<sub>2</sub> – Using 1 MW laser power, spot diameter is 60 mm, with sigma 10 mm, in this case for a 2 m diameter asteroid.

## 5. ORBITAL DEFLECTION MODELING

### 5.1. De-spinning a Rotating Asteroid

With laser ablation technology it is possible to change the spin of an asteroid. The small spot and fine control allow the ability to do precision manipulation on a target. This could be useful in de-spinning an asteroid for capture, landing or mining missions as examples. The time it takes to de-spin an asteroid depends on thrust (torque), initial angular velocity and asteroid diameter. Simple calculations allow calculating the torque necessary to de-spin a rotating spherical solid, assuming homogeneous composition and density. The torque can be varied by changing the power level, changing the spot size or moving the spot to different locations relative to the spin axis:

The torque is  $\tau = F \cdot s$  assuming we apply the force at the edge of the asteroid where  $s = (\text{lever arm}), 0 < s < R$   
 for constant thrust we get constant torque and constant angular acceleration  
 $\omega_{\text{final}} = \omega_0 - \alpha t$  where  $t$  is the desired time to despin the asteroid

$$\omega_0 = \text{initial rotational speed} = \frac{2\pi}{T} \text{ where } T = \text{initial rotation period (s)}$$

$$\text{We want } \omega_{\text{final}} = 0, \text{ hence; } \alpha = \frac{\omega_0}{t} \tag{4.3}$$

$$\text{Assuming a spherical asteroid } I = \frac{2}{5} MR^2$$

$$M = \rho \cdot \frac{4}{3} \pi R^3$$

$$I = \frac{2}{5} \left( \rho \cdot \frac{4}{3} \pi R^3 \right) R^2 = \rho \frac{8\pi R^5}{15} \tag{4.4}$$

$$\text{The required torque is } \tau = I\alpha = \left( \rho \frac{8\pi R^5}{15} \right) \cdot \left( \frac{2\pi}{t \cdot T} \right) = \frac{\rho \cdot 16 \pi^2 R^5}{t \cdot T} \tag{4.5}$$

The required thrust (F) is:

$$F = \frac{\tau}{s} = \left( \frac{8\pi}{15} \rho R^5 \frac{\omega_0}{t} \right) \left( \frac{1}{s} \right) = \frac{\rho \cdot 16 \pi^2 R^5}{s \cdot t \cdot T}$$

Assuming the force is applied at the edge then  $s=R$  and the force required is:

$$F = \frac{\rho \cdot 16 \pi^2 R^4}{t \cdot T} \tag{4.6}$$

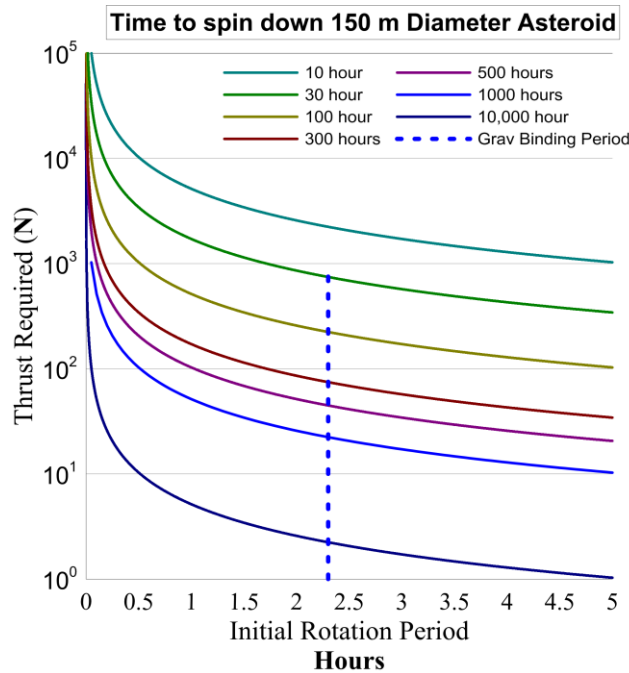


**Figure 8.** Thrust required as a function of rotation period (hours) to de-spin a 150 m diameter asteroid with a density of 2,000 kg/m<sup>3</sup>.

### 5.2. Orbital Propagation Model

Results of a full 3 body (asteroid-Earth-Sun) orbital propagation simulation are shown in Fig 9. Assuming a 0.1 mN/W (optical), this implies a 20 kW laser would be sufficient. A more conservative approach would be to use a significantly

larger laser. This is an extremely efficient approach to mitigation of large asteroids using lasers. One option currently being studied is to repurpose the ARM mission concept where ion engines are used to propel the spacecraft to the asteroid and the laser is used to deflect it. This hybrid approach (ion engines + laser) works extremely well and the system fits within the nominal ARM Block 1 (14 ton to LEO) launch.

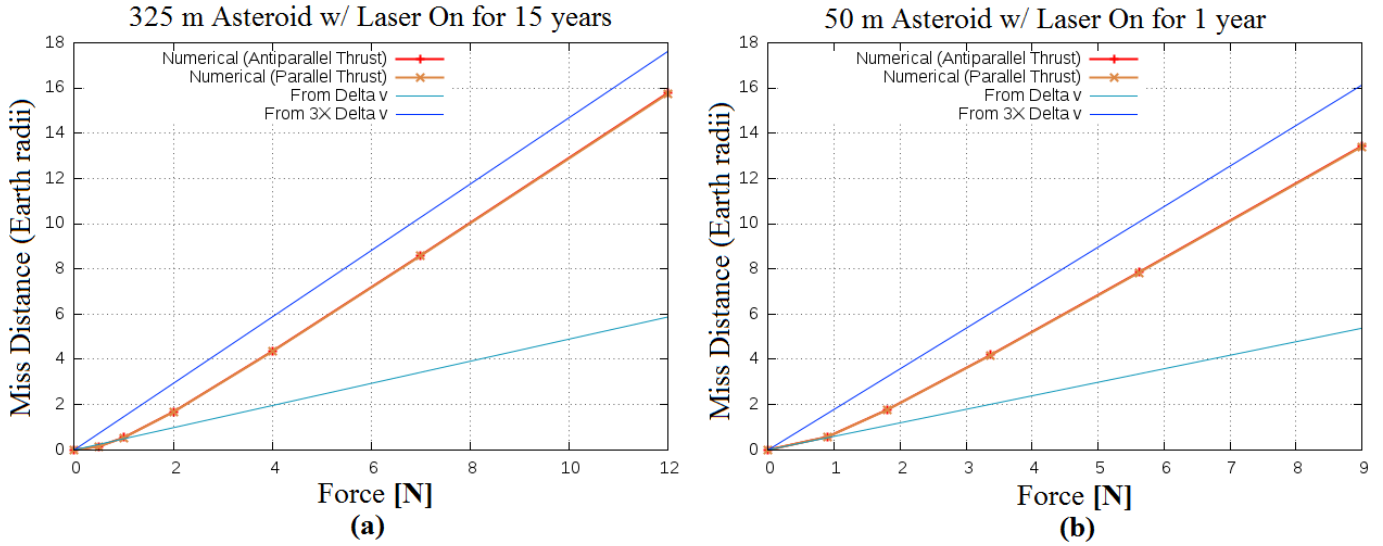


**Figure 9.** Orbital deflection vs. thrust for an Apophis class asteroid with a 325 m diameter and a laser on time of (a) 15 year as well as a (b) 50 m diameter with a laser on time of 1 year. Note the relatively small amount of thrust (~ 2 N in each case) needed to deflect the target by about 2 Earth radii.

### 5.3. Near Term Future Work

- Asteroids that are smaller than ~100 km in diameter are rarely close to spherical. It will be necessary to run simulations that are for non-spherical geometries.
- Run heterogeneous composition models with a rubble surface and regolith like coating.
- Shapes (see Fig. 10) and binary systems: Asteroids like stars, comes in multiplicity (13% NEA's - Near Earth Asteroids/deflected from the main belt). However, binary Asteroids are formed as one single *body*
- Precession, Synchronic, and Chaotic motion

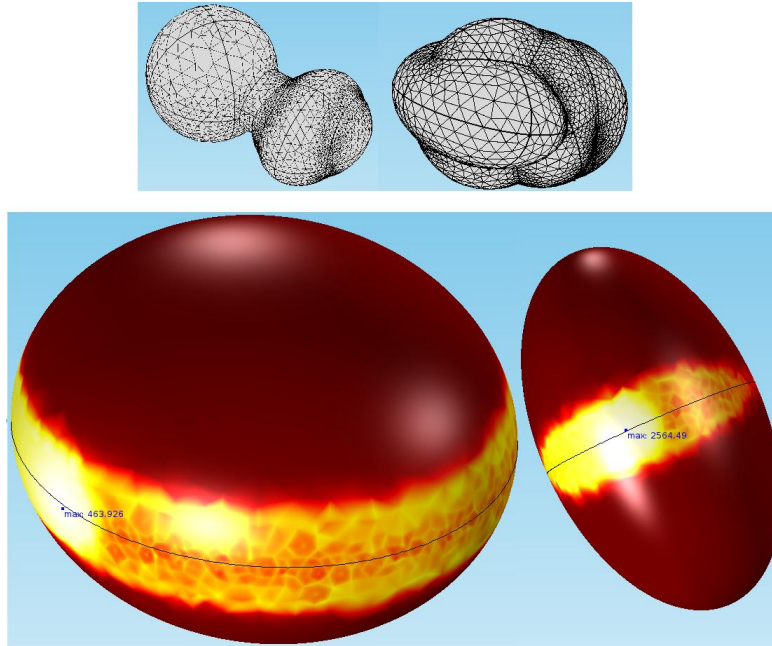


**Figure 10.** Future work will include more complex geometries. Illustrated objects are simulated in COMSOL Multiphysics.

## 6. CONCLUSIONS

The DE-STAR and DE-STARLITE systems provide a feasible solution to asteroids and comets that pose a threat to Earth. By utilizing a directed energy approach with a high powered phase locked laser array to vaporize the target surface the thrust generated from the mass ejection plume is able to propel the asteroid threat away from the original collision trajectory towards Earth. While in orbit around the solar system, asteroids rotate causing the average applied thrust to decrease. A lower limiting rotation period for gravitationally bound objects greater than 150 m is observed to be 2-3 hours consistent with being rubble piles. For periods of the order of hours, there is very little change in the system performance relative to the stationary case, since the plume thrust begins within 1 second after the laser is initiated. Objects with smaller diameters have been observed to be rotating significantly faster but even these do not significantly change the conclusions that a directed energy approach to planetary defense is feasible and compelling. The small DE-STARLITE mission<sup>2</sup> is roughly the size of the proposed ARM mission but is able to mitigate asteroids of more than 300 m diameter as well as de-spin them.

## ACKNOWLEDGEMENTS

We gratefully acknowledge funding from the NASA California Space Grant NASA NNX10AT93H in support of this research.

## REFERENCES

- [1] Lubin, P., Hughes, G.B., Bible, J., Bublitz, J., Arriola, J., Motta, C., Suen, J., Johansson, I.E., Riley, J., Sarvian, N., Clayton-Warwick, D., Wu, J., Milich, A., Oleson, M., Pryor, M., Krogen, P., Kangas, M., and O'Neill, H. "Toward Directed Energy Planetary Defense," *Optical Engineering*, Vol. 53, No. 2, pp 025103-1 to 025103-18 (Feb 2014), doi: 10.1117/1.OE.53.2.025103.
- [2] Kosmo, K., Pryor, M., Lubin, P., Hughes, G.B., O'Neill, H., Meinhold, P., Suen, J., C., Riley, J., Griswold, J., Cook, B.V., Johansson, I., Zhang, Q., Walsh, K., Melis, C., Kangas, M., Bible, J., Motta, Brashears, T., Mathew, S. and Bollag, J. "DE-STARLITE - a practical planetary defense mission," *Nanophotonics and Macrophotonics*

*for Space Environments VIII*, edited by Edward W. Taylor, David A. Cardimona, Proc. of SPIE Vol. 9226 (Aug, 2014).

- [3] Mueller, M., "Surface Properties of Asteroids from Mid-Infrared Observations and Thermophysical Modeling," (2007).
- [4] Mueller, Michael, Alan W. Harris, and Alan Fitzsimmons. "Size, albedo, and taxonomic type of potential spacecraft target Asteroid (10302) 1989 ML." *Icarus* 187.2 (2007): 611-615.
- [5] Harris, A. W., "A Thermal Model for Near-Earth Asteroids," *Icarus* 131, 291-301 (1998).
- [6] Delbò, M., Cellino, A., Tedesco, E. F., "Albedo and Size Determination of Potentially Hazardous Asteroids: (99942) Apophis," *Icarus* 188, 266-270 (2007).
- [7] Margot, J. L., Nolan, M. C., Benner, L. A. M., Ostro, S. J., Jurgens, R. F., Giorgini, J. D., ... & Campbell, D. B. (2002). Binary asteroids in the near-Earth object population. *Science*, 296(5572), 1445-1448 (2002).